JOURNAL OF VIROLOGY, Aug. 2007, p. 7985–7992 Vol. 81, No. 15
0022-538X/07/$08.00+0 doi:10.1128/JVI.00429-07

Minimal Region Sufficient for Genome Dimerization in the Human Immunodeficiency Virus Type 1 Virion and Its Potential Roles in the Early Stages of Viral Replication[▽]

Jun-ichi Sakuragi,* Sayuri Sakuragi, and Tatsuo Shioda

Department of Viral Infections, Research Institute for Microbial Diseases, Osaka University, Osaka, Japan

Received 28 February 2007/Accepted 11 May 2007

It has been suggested that the dimer initiation site/dimer linkage sequence (DIS/DLS) region of the human immunodeficiency virus type 1 (HIV-1) RNA genome plays an important role at various stages of the viral life cycle. Recently we found that the duplication of the DIS/DLS region on viral RNA caused the production of partially monomeric RNAs in virions, indicating that this region indeed mediates RNA-RNA interaction. In this report, we followed up on this finding to identify the necessary and sufficient region for RNA dimerization in the virion of HIV-1. The region thus identified was 144 bases in length, extending from the junction of R/U5 and U5/L stem-loops to the end of SL4. The *trans*-acting responsive element, polyadenylation signal, primer binding site, upper stem-loop of U5/L, and SL2 were not needed for the function of this region. The insertion of this region into the ectopic location of the viral genome did not affect the level of virion production by transfection. However, the resultant virions contained monomerized genomes and showed drastic reductions in infectivity. A reduction was observed especially in the reverse transcription process. An attempt to generate a replication-competent virus with monomerized genome was performed by the long-term culture of mutant virus-infected cells. All recovered viruses were wild-type revertants, indicating a fatal defect of the mutation. These results suggest that genome dimerization or DIS/DLS itself also plays an important role in the early stages of virus infection.

The retrovirus genome is a single-stranded, positive-sense RNA. The viral genome always occurs as a dimer in virus particles, and the interaction is noncovalent since heating easily dissociates purified dimeric genomes into monomers. Template strand switching between two genomes during reverse transcription is often observed in the retroviral life cycle (15). It is likely that the presence of two genomes in one virion helps the virus survive by providing an extra template that can be used when one RNA molecule is damaged and/or providing genetic variety for the progeny. However, this may not fully explain why the virion has to carry two identical RNAs in spite of severe space limitation, so the precise nature of retroviral genome dimerization is still unclear.

The identification of *cis*-acting signals for retrovirus genome dimerization was initially attempted in an in vitro assay (10, 11, 21, 34, 36). Synthesized 5′ RNA fragments of a viral genome, with a length of several hundred to a thousand bases, were found to be dimerized by heating and cooling under suitable buffering conditions. The proposed dimer initiation site/dimer linkage sequence (DIS/DLS) region of human immunodeficiency virus type 1 (HIV-1) is located within the untranslated region between the long terminal repeat (LTR) and the *gag* gene (11, 22). As these regions overlap with a packaging signal, however, it was difficult to perform mutational analysis to study the dimerization of the genome within the virion. Therefore, we recently developed a system to assess the dimerization signal operating within the HIV-1 virion without affecting the packaging ability of the genome (41). This system is an application of our previous finding that duplication of the encapsidation/dimerization signal (E/DLS) region on one RNA genome resulted in the appearance of a monomeric genome in the HIV-1 virion (40). We speculated that an additional E/DLS region at the ectopic position binds to the authentic E/DLS region on the same RNA molecules, thus competitively interfering with intermolecular dimer formation (Fig. 1A). Mutational analysis could thus be utilized to map the DIS/DLS precisely on the HIV-1 RNA. By applying this system, part of the 5′ untranscribed region (UTR) of the HIV-1 genome was examined, and separate functional maps for dimerization and encapsidation signals could be created. By comparing these two maps, we concluded that RNA dimer linkage formation must be an essential process in genome packaging, which consists of multiple sequential steps (41). In the study reported here, we employed our original system to identify the region which is necessary and sufficient for HIV-1 genome dimerization in the virion. We also report on our further investigation of the roles of the dimerization signal at various stages of viral replication and discuss the possibility that it may perform functions other than genome packaging in the viral life cycle.

MATERIALS AND METHODS

DNA constructs. The replication-competent HIV-1 proviral clone pNL4-3 (2) and pMSMBA (23), a derivative of pNL4-3, were used as progenitors for the mutant constructs described here. Mutant plasmids were constructed with standard methods. To construct pDDNT4, pDDNU4, and pDDNL4, three pairs of primers were first used for PCR amplification of the HIV-1 leader region by using the plasmid pGEM-MM (40) as a template. The first pair comprised the sense primer TarF (5′-GGTCTCTCTGGTTAGACCAG-3′) and the antisense primer SL4Rs (5′-GACGCTCTCGCACCCATC-3′), the second pair consisted of the sense primer R/U5F (5′-CACTGCTTAAGCCTCAACGATCG-3′) and the antisense primer SL4Rs, and the third pair consisted of the sense primer

* Corresponding author. Mailing address: Department of Viral Infections, Research Institute for Microbial Diseases, Osaka University, 3-1 Yamadaoka, Suita City, Osaka 565-0871, Japan. Phone: 81-6-6879-834. Fax: 81-6-6879-8347. E-mail: sakuragi@biken.osaka-u.ac.jp.

▽ Published ahead of print on 15 May 2007.

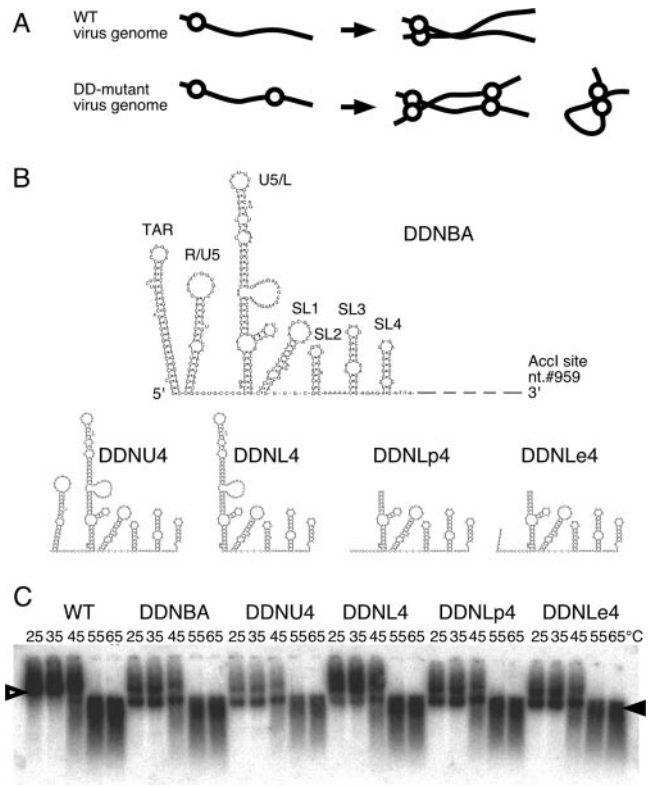

FIG. 1. The 5′ and 3′ ends of a functional domain of DLS. (A) A schematic image of monomer formation of the E/DLS duplicated mutant (DD-mutant) genome. Genomes of the WT virus form dimers, whereas those of DD-mutant form both dimers and monomers. Solid lines and open circles represent viral genome RNA and E/DLS, respectively. (B) Possible two-dimensional folds of the inserted fragment of each of the constructed mutants. nt., nucleotide. (C) Virion RNA profiles in native agarose gel. Viruses were prepared by transfection of 293T cells with pNLNh (WT) or its derivative mutants. At 48 h posttransfection, culture supernatants were harvested. Virions in the supernatant were collected by ultracentrifugation through a 20% sucrose cushion for isolation of the virion RNA. Open and solid arrowheads denote positions of dimers and monomers, respectively.

U5/LF (5′-TCTGTTGTGTGACTCTGGTAAC-3′) and the antisense primer SL4Rs. The three amplified fragments were isolated and ligated in pGEM-Teasy (Promega, Madison, WI) to generate pGEMT4sub, pGEMU4sub, and pGEML4sub, respectively. The digestion of these plasmids with EcoRI, blunt ended by T4 DNA polymerase, resulted in the isolation of approximately 300-bp fragments, including the 5′ leader region of HIV-1. These fragments were then ligated into the T4 DNA polymerase-treated NheI site of pNL4-3 to construct pDDNT4, pDDNU4, and pDDNL4, respectively. The orientation of the inserted fragments was verified by sequencing. pDDNLp4 and pDDNLe4 were constructed in a similar way, except for the use of pdLA3 (39) as a PCR template and different sense primers. The sense primer for pDDNLp4 was A3F+N (5′-TGTGCCCGTCTGTTGTGTGACTC-3′), and that for pDDNLe4 was A3U5endN (5′-AGTAGTGTGTGCCCGTCTGTTGTGTGACTC-3′). To construct pDDNLp4Δ1 and pDDNLp4Δ3, pdM and pdX (25) were used as templates for PCR amplification with the sense primer LpLA3 (5′-TGTGCCCGTCTGTTGTGTGACTCTGGTGCCAGAGGAG-3′) and the antisense primer SL4Rs, respectively. The two amplified fragments were isolated and ligated in pGEM-Teasy to generate pGEMLp4Δ1sub and pGEMLp4Δ3sub, respectively. To construct pDDNLp4Δ2, two-step PCR amplification was performed by using pGEMLp4sub as a template. The first pair of primers comprised the sense primer A3F+N and the antisense primer dS2R (5′-CAAAATTTTTGCCCCTCGCC-3′), and the second pair comprised the sense primer dS2F (5′-GGCGAGGGGCAAAAATTTTG-3′) and the antisense primer SL4Rs. Two amplified fragments were isolated, mixed, and used for the second PCR with primers A3F+N and SL4Rs to generate a mutated fragment. This fragment was then isolated and ligated in pGEM-Teasy to generate pGEMLp4Δ2sub. To construct pDDNLp4Δ4, pGEMLp4sub was used as a template for PCR amplification with the sense primer A3F+N and the antisense primer dS4 (5′-CATCTCTCCTTCTAGCC-3′). The amplified fragment was isolated and ligated in pGEM-Teasy to generate pGEMLp4Δ4sub. The digestion of pGEMLp4Δ1sub, -Δ2sub, -Δ3sub, and -Δ4sub with EcoRI, blunt ended by T4 DNA polymerase, resulted in the isolation of fragments, including the 5′ leader region of HIV-1. These fragments were then ligated into the T4 DNA polymerase-treated NheI site of pNL4-3 to construct pDDNLp4Δ1, -Δ2, -Δ3, and -Δ4, respectively. The EcoRI fragment from pGEMLp4Δ2sub (fragment Lp4Δ2) was blunt ended by T4 DNA polymerase and ligated into the BsaBI site of pDDNLp4Δ2 to create pDTNLp4Δ2. The plasmid p5′ssβglob (24) features a deletion on the 5′ untranslated region of pMSMBA (nucleotides 694 to 783) and an insertion at the point of deletion of a portion of the sequence spanning the 5′ splicing signal of the first intron of the β-globin gene. The 2.2-kb StuI-XhoI fragments containing env regions of pDDNLp4Δ2 and pDTNLp4Δ2 were inserted into the corresponding position of p5′ssβglob to create pssNLp4Δ2 and psTNLp4Δ2, respectively. The fragment Lp4Δ2 was blunt ended by T4 DNA polymerase and ligated into the T4 DNA polymerase-treated XhoI site of pNL4-3 to construct pDDXE+. The fragment Lp4Δ2 was ligated into the EcoRI site of pNL4-3 to construct pDDEE+. pDDEE+ was digested with Sse8387I, and NheI, a 4.4-kb, *pol-env* region-containing fragment, was isolated and exchanged at the same position of pDDXE+ to construct pDTEXE+. The construction of the HIV-2 *env* expression vector, pCGH2env, has been described previously elsewhere (28).

DNA transfection. 293T cells (13) (approximately 3×10^6) were seeded on dishes (diameter, 100 mm) the day before transfection with plasmid DNA (5 μg) by means of the calcium phosphate precipitation method (3). The day after transfection, the supernatant was replaced with fresh medium.

Virus infection. At 48 to 72 h posttransfection, the medium was centrifuged and the supernatant was used for infection with inoculation of equal amounts of CA-p24 into MT-4, M8166, or M8166/H1Luc cells (27). The supernatants of MT-4 or M8166 were harvested every 3 or 4 days for the multiple replication assay, while 10 μl of each cell supernatant was analyzed with the exogenous reverse transcriptase (RT) assay as described previously (43). M8166/H1Luc cells contain integrated reporter DNA carrying the HIV-1 LTR and luciferase. Upon infection with HIV-1, the HIV-1 LTR is activated along with the expression of viral transactivator Tat and luciferase expression in cytoplasm is induced. The same amount of CA-p24 recovered from each construct was inoculated into M8166/H1Luc cells, and luciferase expression within the cells was measured 24 h after infection. The luciferase assay was performed with the Bright-Glo luciferase assay system (Promega).

Isolation of RNA from virions. At 48 to 72 h posttransfection, virus particles were collected concurrently from medium as described previously elsewhere (23). The physical virus titer was determined with an enzyme-linked immunosorbent assay kit to quantitate CA-p24 (ZeptoMetrix, Inc., Buffalo, NY). To isolate RNA from particles, virions were disrupted by the addition of 1% sodium dodecyl sulfate and treated with proteinase K (300 μg/ml) at room temperature for 60 min, followed by Tris-EDTA-saturated phenol-chloroform extraction, chloroform extraction, and ethanol precipitation.

Northern blotting analysis. Pelleted RNA was resuspended in T buffer (10 mM Tris-HCl, pH 7.5, 1 mM EDTA, 1% sodium dodecyl sulfate, 100 mM NaCl, and 10% formamide), and the thermostability of dimeric viral RNA was determined by incubating RNA aliquots for 10 min at the temperatures indicated (42). RNA electrophoresis on native agarose gel and Northern hybridization analysis were performed as described previously elsewhere (41). Plasmid T7pol (42) was used to synthesize a cRNA probe for Northern hybridization. In experiments designed to assess the conversion of dimers to monomers, relative amounts of both RNA species were quantitated by PhosphorImager analysis (Fujifilm Co., Tokyo, Japan) and ratios of dimers and monomers were determined.

RNase protection assay. The antisense probe ($\sim 10^8$ cpm/mg) specific to the NL4-3 *gag* region was synthesized by in vitro transcription. One-fifth of the virion-associated RNA was mixed with 8×10^4 Cerenkov counts of ^{32}P-labeled antisense riboprobe and precipitated with ethanol. RNase protection assays were performed with an RPA III RNase protection assay kit (Ambion, Inc., Austin, TX). After electrophoresis in 5% polyacrylamide-8 M urea gels, protected RNA was quantitated by PhosphorImager analysis (Fujifilm Co.).

Real-time PCR analysis. At 48 to 72 h posttransfection, culture supernatants of the transfected cells were harvested. The supernatants were treated with DNase prior to infection to eliminate plasmid DNA contamination as described previously elsewhere (20) and inoculated into 10^6 MT-4 cells. For PCR analysis, total DNA was extracted from infected cells 20 h after infection by using a GenElute mammalian genomic DNA miniprep kit (Sigma, St. Louis, MO).

TABLE 1. Packaging efficiency of the mutants analyzed[a]

Mutant or WT	Avg ± SEM
WT	1 ± 0
DDNT4	0.84 ± 0.14
DDNU4	1.61 ± 0.26
DDNL4	1.09 ± 0.10
DDNLp4	1.04 ± 0.08
DDNLe4	0.94 ± 0.09

[a] The values were calculated by dividing the quantity of viral RNA by that of CA-p24. The value of WT (NLNh) was set at 1. Values are averages of results of at least three independent experiments.

Real-time PCR was performed with an Applied Biosystems 7500 real-time PCR system to quantitate viral cDNA synthesis during infection. Primers and TaqMan probes were selected according to criteria described previously elsewhere (19), and samples (0.5 μg DNA) were subjected to 40 cycles of PCR in a 10-μl reaction mixture. A series of known amounts of plasmid DNA were amplified along with total DNA to serve as a standard in each experiment. For the quantitation of the 2-LTR from virus DNA, a 2-LTR circle junction was cloned into pGEM-Teasy plasmid (Promega) as a TA cloning fragment by PCR amplification from 2-LTR circles, with total DNA extracted from infected MT-4 cells serving as a template. Serial dilutions of this plasmid were used as a standard to determine copy numbers of 2-LTR circles in the samples in the same manner as that for the determination of other DNA copy numbers.

For integrated proviral DNA quantitation, a modification of a recently reported Alu PCR method (7, 18) was employed (28). In short, two outward-facing Alu primers that anneal within the conserved regions of the Alu repeat element were used, together with an HIV-1 LTR-specific primer (L-M667), to optimize the probability of amplifying an LTR sequence for the first round of PCR. For the second round of PCR (real-time PCR), a lambda-specific primer (Lambda T) was used as a sense primer to detect only the amplified fragments in the first round of PCR and a TaqMan probe and an antisense primer were selected from the previous set for R/U5 DNA detection (19). The resultant PCR products were diluted 100-fold and subjected to real-time PCR.

RESULTS

The 5′ and 3′ ends of a functional domain of DIS/DLS. In a previous study of ours, the minimal RNA region required for RNA dimerization in virions was identified as a fragment inserted in the *env* region of pDDNBA (41). The fragment was approximately 500 bases long, extending from the 5′ capping site to the middle of the MA gene of the viral genome with deletion of the polyadenylation signal and primer binding site (PBS). We first constructed five mutants to precisely map the 5′ and 3′ ends of the functional region of DIS/DLS (Fig. 1). The viral genome packaging efficiency of all mutants was similar to that of the wild type (WT), indicating that the mutations had little effect on packaging ability (Table 1). The viral genome from mutant DDNT4, which contains an ectopic fragment (334 bases, from the *trans*-acting responsive element [TAR] to SL4) at the *env* region, formed a monomer very similar to that of the original mutant DDNBA (monomer content was more than 40% of the total viral genome in native condition), which indicated that sequence 3′ to SL4 was not needed for mediating RNA-RNA interactions in virions (data not shown). pDDNU4 carried a fragment from the R/U5 [poly(A)] stem-loop to SL4 (277 bases), and pDDNL4 carried a fragment from the U5/L stem-loop to SL4 (222 bases). As shown in Fig. 1B, the viral genome from DDNU4 formed a monomeric RNA comparable to DDNBA (monomer content was more than 40%), whereas the viral genome from DDNL4 formed a monomeric RNA with a greatly reduced amount of monomer (<20%). These results indicate that the 5′ end of the functional region of DIS/DLS was lost from DDNL4. We therefore added 8 and 15 nucleotides of the 5′ sequences to DDNL4 to generate DDNLp4 and DDNLe4, respectively. An upper stem-loop and PBS of the U5/L region were deleted from the inserted fragment of DDNLp4 and DDNLe4 because our previous data showed that those parts were dispensable for the dimer linkage formation function (41). Both viral RNAs of DDNLp4 and DDNLe4 formed a genome with a monomeric content (>40%) comparable to that of the WT in the virion (Fig. 1B). Taken together, these findings suggest that the region from the R/U5-U5/L junction to SL4 is sufficient to produce dimeric RNA in virions.

Minimal region sufficient for RNA dimerization is 144 bases long. We then examined the involvement in dimer linkage formation of four stem-loops, SL1 (putative "DIS"), SL2 (splicing signal), SL3 (essential region of packaging signal), and SL4 (containing *gag*AUG). Four mutants, DDNLp4Δ1, DDNLp4Δ2, DDNLp4Δ3, and DDNLp4Δ4, were constructed as derivatives of DDNLp4. Each mutant contained a deletion of one of four stem-loops on the ectopic fragment of DDNLp4 (Fig. 2A). As shown in Fig. 2B, only DDNLp4Δ2 formed a monomeric genome similar to the one derived from DDNBA,

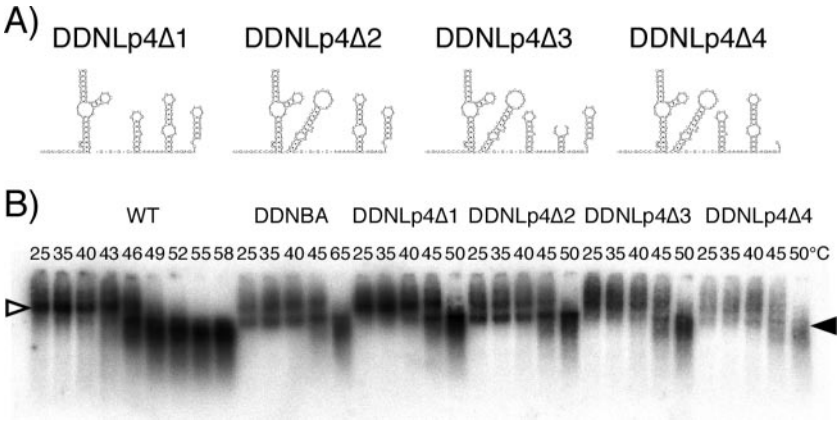

FIG. 2. Determination of the necessary and sufficient DLS in virions. (A) Probable two-dimensional folds of the inserted fragment of each of the constructed mutants. (B) Virion RNA profiles in native agarose gel. Virion RNA was isolated, and Northern hybridization was performed as described for Fig. 1. Open and solid arrowheads denote positions of dimers and monomers, respectively.

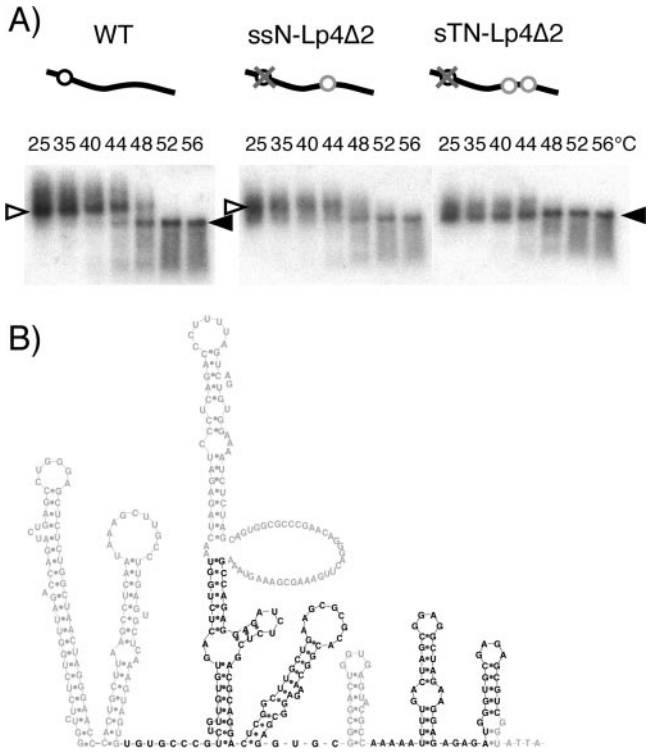

FIG. 3. Verification of the minimal DLS for its ability to induce RNA-RNA interaction in HIV-1 virions. (A) Virion RNA profiles in native agarose gel. Virion RNA was isolated, and Northern hybridization was performed as described for Fig. 1. Open and solid arrowheads denote positions of dimers and monomers, respectively. Schematic diagrams of mutants are shown above the blots. Solid lines, open circles, gray circles, and gray crosses represent viral genome RNA, authentic E/DLS, Lp4Δ2 fragments, and mutations introduced to knock out E/DLS functions, respectively. (B) A schematic Mfold representative of the verified area.

whereas other mutants displayed low levels of monomeric genome formation in virions. This indicates that the major splicing donor, SL2, is dispensable for RNA-RNA interaction, while the three other stem-loops are necessary for dimer linkage formation in virions.

In a previous study, we constructed two mutants, ssN− and sTN−, which contained a deletion of authentic DIS/DLS and an insertion of one (ssN−) or two (sTN−) DIS/DLS fragments in the ectopic position of the viral genome (39). Viral genomes from dimers formed from ssN− were similar to the WT, and nearly all viral genomes in virions of sTN− were monomers. This suggests that the two fragments inserted on one RNA strand interacted exclusively and intramolecularly with each other to prevent intermolecular dimerization. To confirm that fragment Lp4Δ2 was necessary and sufficient for RNA dimer linkage formation in virions, we constructed two mutants, ssNLp4Δ2 and sTNLp4Δ2, in the same way that ssN− and sTN− were constructed, except for the use of fragment Lp4Δ2 for insertion. As we expected, viral genomes from ssNLp4Δ2 formed dimers similar to those of the WT, while the viral genome from sTNLp4Δ2 exclusively formed monomers (Fig. 3A). Thus, the Lp4Δ2 fragment, 144 bases in length, was necessary and sufficient for mediating RNA dimerization in HIV-1 virions (Fig. 3B).

Single-round infection efficiency of HIV-1 mutant containing monomeric genome. We previously demonstrated the particle formation of HIV-1 which contained exclusively monomerized genome (39). This suggested that whole-genome dimerization is not essential for RNA packaging and particle formation of the viral genome, although dimer linkage formation of the DLS region is essential for these functions (41). On the other hand, no efficient infection or replication of HIV-1 mutants containing a monomeric genome was observed since significant reduction of intact viral DNA production occurred as a result of aberrant strand transfer and/or recombination during reverse transcription (39). Strand transfer during the reverse transcription process of the retroviral genome targets the R region of the viral LTR (12), which has also been suggested to be a hot spot for recombination (26). The production of aberrant viral cDNA products could thus be induced by the presence of multimerized R regions on the genome of the mutants. Since Lp4Δ2, the minimum DLS we identified here, did not include any R region, its ability to induce aberrant strand transfer and/or recombination by duplication of Lp4Δ2 in the viral genome was expected to be reduced. We therefore compared the single-round replication efficiencies of mutants DDNLp4Δ1, -Δ2, -Δ3, and -Δ4 pseudotyped with the HIV-2 envelope. The result demonstrated that all mutants containing Lp4 fragments showed reduced infectivity, which may be the effect of homologous recombination at a sequence-duplicated location (Fig. 4A). However, the infectivity of DDNLp4Δ2, the only mutant packaging monomeric genome, was three- to five-fold lower than that of other mutants. As the M8166/H1Luc cell assay reflects the magnitude of Tat expression of the samples, this result suggests that the mutations introduced in these constructs affect mainly the step(s) between virus penetration and early gene expression.

Reverse transcription predominantly blocked in monomeric genome mutants. To determine the step(s) in the viral replication cycle affected by the mutation described above, we analyzed the efficiency of each of the replication steps of the mutants. We chose two mutants, DDNLp4Δ2 and -Δ3, for comparison, since they are very similar in length of duplicated sequences but quite different in infectivity. We analyzed the virion production and viral RNA encapsidation ability of the mutants by purifying the virion and viral RNA from the supernatant of transfectant 293T cells. As shown in Fig. 4B, both functions of the mutants were similar or only moderately reduced compared to those of the WT, indicating that the mutations had little effect on these processes.

We next quantitated the levels of virus reverse-transcribed products, 2-LTR viral circular DNA, and integrated viral DNA using real-time PCR. HIV-2 *env*-pseudotyped virus was generated by transfection and purified, and equivalent amounts of CA-p24 were used to infect MT-4 cells. At 20 h after infection, total DNA was isolated from virus-infected cells. To examine the progress of reverse transcription, four sets of primers and probes were prepared (see Materials and Methods) and used to measure the synthesis of the strong-stop negative-strand DNA, first-strand transferred DNA, *gag* region DNA, and second-strand transferred DNA within total cellular DNA. Figure 4C shows the organized results of viral DNA quantitation.

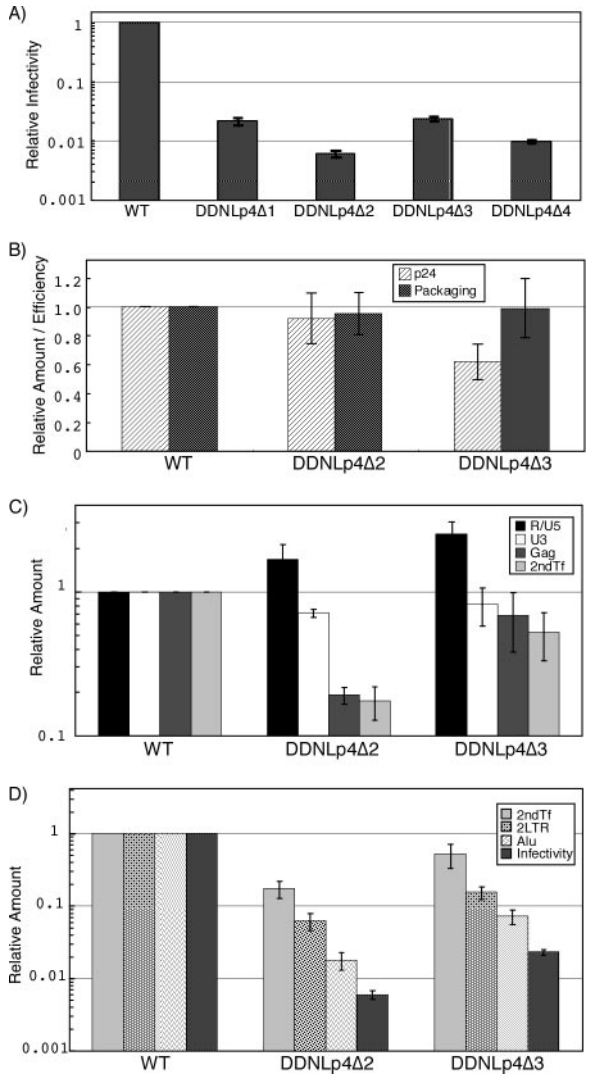

FIG. 4. Infectivity of mutant viruses. For each graph, the value of the WT was set at 1. Figures show the averages of results of at least two independent experiments. Error bars represent standard errors. (A) Single-round replication assay. M8166/H1Luc cells (1×10^6) were infected with the same quantity of CA-p24 of WT or mutant viruses pseudotyped with HIV-2 Env. At 24 to 48 h postinfection, cells were lysed and luciferase activity in the cell lysate was measured. (B) CA-p24 production and RNA packaging ability. Quantities of CA-p24 and viral RNA of purified virions were measured with the enzyme-linked immunosorbent assay and the RNase protection assay, respectively. Packaging efficiency was calculated by dividing the quantity of viral RNA by that of CA-p24. (C and D) Viral DNA quantification at early infection steps. A total of 1×10^6 MT-4 cells were infected with the same quantity of CA-p24 of WT or mutant viruses pseudotyped with HIV-2 Env. At 20 h postinfection, total cellular DNA was extracted and treated with DpnI overnight to digest methylated plasmid DNA. An equal amount of DNA was subjected to real-time PCR analysis. R/U5, strong-stop DNAs; U3, first-strand transferred products; Gag, negative-strand late products; 2ndTf, second-strand transferred products; 2LTR, 2-LTR viral circular DNA; Alu, PCR quantification for integrated proviral DNA; Infectivity, M8166/H1Luc cell assay as described for Fig. 4A.

Compared to the WT, a moderately large amount of DNA of both mutants was observed at the point of strong-stop DNA synthesis, which was reduced to a level similar to that of the WT in the subsequent first-strand transfer. At the next step, a big difference between the two mutants was observed. During the elongation of negative-strand DNA, the level of DNA synthesis of the DDNLp4Δ2 mutant was reduced to about 20%, whereas that of the DDNLp4Δ3 mutant remained at more than 60%. The level of DNA after the second-strand transfer showed additional moderate reduction for both of the mutants. As a result, a less than 50% reduction in overall viral cDNA production was observed in the DDNLp4Δ3 mutant, but a more than 80% reduction was observed in the DDNLp4Δ2 mutant. This result suggests that one of the defects was present at the reverse transcription stage. The reduction of the amounts of 2-LTR DNA, integrated DNA, and the infectivity are essentially similar between two mutants (Fig. 4D). As the 2-LTR circular DNA can be used as an indicator of RT completion and nuclear import of viral DNA (19), our findings suggest that the replication process from nuclear import to early gene expression was not specifically affected in a dimerization-defective mutant.

Attempt to generate replication-competent HIV-1 mutant containing monomeric genome. Multiround replication of a defective mutant virus sometimes results in the appearance of compensatory mutations to recover infectivity of the mutant without affecting viral RNA stability (38). Although we could not detect any efficient infectivity of mutant DDNLp4Δ2, we thought it might be possible to generate a replication-competent HIV-1 mutant containing a monomeric genome by means of long-term culture of infected cells. To verify this possibility, we constructed three mutants with Lp4Δ2 fragments on their genome, which retained all essential genes (*gag*, *pol*, *env*, *tat*, and *rev*) and important accessory genes (*vif* and *vpu*) but packaged the monomeric genome. Fragment Lp4Δ2 was inserted into *vpr*, *nef*, or both of pNL4-3 to construct pDDEE+, pDDXE+, and pDTEXE+, respectively (Fig. 5A). 293T cells were transfected with these constructs, the culture supernatants were harvested 2 to 3 days later, and the released virions collected. Roughly, the level of virion production by all three mutants was similar to that of the WT (data not shown). The genome from mutant virions contained 30 to 50% of monomeric genomes as shown by native Northern blotting analysis, thus confirming our previous observation (Fig. 5C). The mutants were examined for their ability to replicate in human $CD4^+$ cell lines MT-4 and M8166. Figure 6B shows the growth kinetics of the mutants in MT-4 cells. Mutant DTEXE+ was replication defective in MT-4 cells, while two mutants, DDEE+ and DDXE+, showed detectable virus replication but with growth kinetics that were significantly reduced and delayed compared to those of WT. On the other hand, all mutants were replication negative in M8166 cells (data not shown). Replicated viruses in the culture supernatant of MT-4 were harvested at their kinetic peak point. Equal amounts of RT units of virus samples were used for assay of reinfection of MT-4 cells, the remainder was centrifuged to purify virions, and the viral genome RNA was isolated. Growth kinetics of reinfected mutants restored their replication ability to a level comparable to that of the WT, suggesting that they had become revertants (data not shown). The results of native Northern blotting of genome RNA showed that MT-4 replicating mutants formed mostly dimers similar to that of the WT (Fig. 5D). Proviral genome sequencing from infected MT-4 chromosomal DNA proved that Lp4Δ2 sequences inserted in ectopic positions of the genome

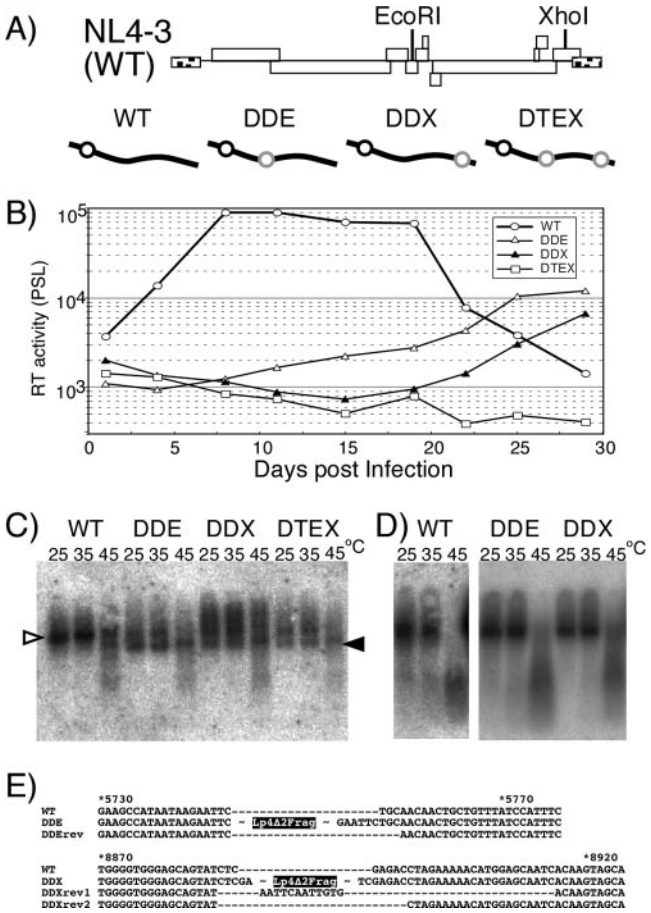

FIG. 5. Replication assay of mutants carrying a monomeric genome. (A) Schematic diagrams of replication-competent form mutants. The positions of restriction enzyme sites on the viral genome used for insertion are shown in the upper part of the panel. Diagrams of the mutants are shown in the lower part of the panel. Symbols are the same as those described for Fig. 3. (B) Growth kinetics of viruses. Values are representative of the results of at least three independent experiments. Viruses were prepared by transfection of 293T cells with pNL4-3 (WT) or its derivative mutants (pDDEE+ [DDE], pDDXE+ [DDX], and pDTEXE+ [DTE]). At 48 h posttransfection, culture supernatants of transfected 293T cells were harvested, and equal quantities of CA-p24 were inoculated into MT-4 cells. The supernatants of the cells were harvested every 3 or 4 days. Ten microliters of each cell supernatant was subjected to exogenous RT assay and quantitated by PhosphorImager analysis. PSL, Photostimulierte Lumineszenz. (C) Virion RNA profiles produced from transfected 293T cells and visualized by native Northern blotting analysis. Open and solid arrowheads denote positions of dimers and monomers, respectively. (D) Virion RNA profiles produced from MT-4 cells. Viruses were harvested at their growth kinetic peak point (wild type, 10 days postinfection; DDE and DDX, 28 days postinfection). (E) The nature of reversions. The sequences in the vicinity of the fragment-inserted sites are shown. The names of revertant sequences include "rev." The positions of Lp4Δ2 fragment insertion of DDE and DDX are indicated. The numbers above the sequences represent nucleotide positions of pNL4-3 (WT).

were completely deleted from both replication-competent mutants (Fig. 5E). Since the sequences of the revertants were found to contain an additional deletion or a small part of the inserted sequence at the mutated positions (Fig. 5E), the possibility of WT virus contamination could be ruled out.

DISCUSSION

The recent growth in interest in retrovirus genome dimerization has resulted in many publications that deal with its various aspects and that vary in depth and breadth (for reviews, see references 31, 35, and 37) Nonetheless, the overall picture of the retroviral dimerization signal remains unclear, so that there is still a need for detailed examination. The aim of the study reported here was to identify the minimal region sufficient for genome dimerization of HIV-1 in virions. In the first set of experiments, we defined the region sufficient for dimer linkage formation, and, in a subsequent experiment, we generated several deletion mutants to determine the minimal DLS required for HIV genome dimer linkage formation in virions. The minimal DLS identified in this study was only 144 bases long and included SL1, SL3, and SL4. Especially, SL1 deletion is more deleterious than is deletion of the other elements for dimer linkage formation in Fig. 2. It has been suggested that the hairpin loop of SL1 in DLS, known as DIS, plays a crucial role in dimerization and recombination (9, 33, 41). Our findings are well consistent with this notion.

While there are many functional regions for viral viability in the 5′ UTR of HIV, such as TAR, polyadenylation signal, PBS, and splicing donor, none was required for the dimerization function. This suggests that the genome dimerization of HIV-1 is independent of transactivation, splicing, or primer annealing. As we pointed out in a previous paper of ours (41) and in this study, the lower stem of the U5/L stem-loop is required for dimerization, which was not clearly identified during in vitro studies (for a review, see reference 30). This stem contains a so-called primer activation signal (5), which is thought to activate the initiation of reverse transcription. Since PBS or primer annealing is not required for dimerization, the involvement of primer activation signal and its opposing stem sequence in dimerization may be limited simply to creating a stable structure. Several studies have suggested that TAR, the R-U5 stem-loop region or coding region of *gag*, participates in the dimerization (4, 14, 16, 32) The contribution of those regions to RNA dimerization was demonstrated mainly in in vitro assays, but they were not included in the DLS identified in the in vivo assay used in our study. However, the possibility of a contribution by these regions cannot be ruled out since all mutants in our study retained the intact 5′ UTR. This result means that all mutants possess at least one set of the regions in the original position per genome, so that they may perform certain incidental functions for dimerization in virions.

Mfold RNA stability calculation (44) showed that the junction between R/U5 and U5/L stem-loops is relatively "free," which suggests that it is not involved in a base-pairing interaction with vicinal sequences (Fig. 1A). However, recent reports have suggested that the HIV-1 genome leader region could form an alternative structure known as the branched multiple hairpin (BMH) (1, 17). In this model, the 5′ junction sequence forms a stem structure with a sequence at the 3′ end of DLS. Although the BMH model was validated in an in vitro experiment, the DLS we defined in vivo was found to include all sequences required for the BMH formation. As an interaction between 5′ and 3′ ends of DLS should be essential for BMH formation, we evaluated the importance of both ends in vivo by making several base substitution mutants. The mutants con-

tained four to eight-base substitutions in either or both ends of the Lp4Δ2 fragment inserted in pDDNLp4Δ2. As expected, the 5′ or 3′ region of DLS appeared to be very important in dimer linkage formation of RNA since at least four-base substitutions (four substitutions in 8 bases of the 5′ end or four substitutions in 15 bases of the 3′ end) seriously disrupted the function (data not shown). Nonetheless, our attempt failed to yield a clear answer to whether BMH structure exists in virion RNA, probably because of difficulty in estimating the effect of the mutations on actual RNA shape in this region.

A noteworthy result of the M8166/H1Luc cell assay, an infectivity assay of monomeric genome mutants, was that the overall single-round infectivity of the mutant DDNLp4Δ2 was dramatically reduced (Fig. 4A). In our previous study, we reported that another monomeric genome mutant, DDNΔPBS, produced virions with less than 1% of infectivity of the WT (in one representative experiment, 1.4 versus 187.5 β-galactosidase-inducing units per ng of CA-p24 in a multinuclear activation of galactosidase indicator cell assay) (39). It well coincided with the data we got in the present study. As the inserted fragments of the four mutants were very similar in length and sequence (DDNLp4Δ1, 128 bases; DDNLp4Δ2, 144 bases; DDNLp4Δ3, 149 bases; and DDNLp4Δ4, 149 bases), a prominent replication defect of DDNLp4Δ2 might correlate with the appearance of monomeric genomes in virions, which is a unique feature of this mutant. Stepwise measurement of replication efficiency identified defects of the mutants in multiple steps of infection (Fig. 4C and D). Levels of viral DNA synthesis of DDNLp4Δ2 fell to around 15% of WT, whereas more than half of its viral DNA synthesis ability was retained in the DDNLp4Δ3 mutant. This difference strongly suggests a negative effect of the monomeric genome on reverse transcription. As the monomeric genome in virions of DDNLp4Δ2 accounted for 50% or less (Fig. 2B) of their content, the defect shown here occurred not only on the monomeric genome but also on the normal-looking dimeric genome of the mutants. These results seem to indicate that the inserted fragment of the mutant caused an abnormal secondary or tertiary structure of the overall viral RNA genome, resulting in poor reverse transcription. Viral genome dimerization and/or DIS was reported to play a role in efficient reverse transcription (6, 29), and our data supported these earlier arguments.

A multiround infection experiment clearly demonstrated significantly reduced growth kinetics of the mutants (Fig. 5). Moreover, inserted sequences of the mutants were completely deleted during the replication process, which strongly suggests that the insertion caused a fatal defect in viral replication. The appearance of revertants before the occurrence of compensation mutation implies that aberrant viral RNA conformation in these mutants was too drastic to be undone by protein modification.

In conclusion, in this study, we succeeded in identifying the essential region for HIV-1 genome dimer linkage formation in virions. Our consecutive experiments demonstrated that the dimerization region on RNA molecules may be important for the efficient progress of reverse transcription, probably by maintaining an appropriate form of viral genome in virions. A recent study has suggested that HIV-1 *pol* proteins contribute to genome RNA dimerization (8), which could be related to our speculation. Further studies can be expected to provide more findings relevant to this hypothesis.

ACKNOWLEDGMENTS

This work was supported by grants from the Ministry of Education, Culture, Sports, Science and Technology; the Ministry of Health, Labor, and Welfare; and the Health Science Foundation of Japan.

REFERENCES

1. **Abbink, T. E., and B. Berkhout.** 2003. A novel long distance base-pairing interaction in human immunodeficiency virus type 1 RNA occludes the Gag start codon. J. Biol. Chem. **278:**11601–11611.
2. **Adachi, A., H. E. Gendelman, S. Koenig, T. Folks, R. Willey, A. Rabson, and M. A. Martin.** 1986. Production of acquired immunodeficiency syndrome-associated retrovirus in human and nonhuman cells transfected with an infectious molecular clone. J. Virol. **59:**284–291.
3. **Aldovini, A., and B. D. Walker.** 1990. Techniques in HIV research. Stockton Press, New York, NY.
4. **Andersen, E. S., S. A. Contera, B. Knudsen, C. K. Damgaard, F. Besenbacher, and J. Kjems.** 2004. Role of the trans-activation response element in dimerization of HIV-1 RNA. J. Biol. Chem. **279:**22243–22249.
5. **Beerens, N., F. Groot, and B. Berkhout.** 2001. Initiation of HIV-1 reverse transcription is regulated by a primer activation signal. J. Biol. Chem. **276:**31247–31256.
6. **Berkhout, B., A. T. Das, and J. L. van Wamel.** 1998. The native structure of the human immunodeficiency virus type 1 RNA genome is required for the first strand transfer of reverse transcription. Virology **249:**211–218.
7. **Brussel, A., and P. Sonigo.** 2003. Analysis of early human immunodeficiency virus type 1 DNA synthesis by use of a new sensitive assay for quantifying integrated provirus. J. Virol. **77:**10119–10124.
8. **Buxton, P., G. Tachedjian, and J. Mak.** 2005. Analysis of the contribution of reverse transcriptase and integrase proteins to retroviral RNA dimer conformation. J. Virol. **79:**6338–6348.
9. **Chin, M. P., T. D. Rhodes, J. Chen, W. Fu, and W. S. Hu.** 2005. Identification of a major restriction in HIV-1 intersubtype recombination. Proc. Natl. Acad. Sci. USA **102:**9002–9007.
10. **Darlix, J. L., C. Gabus, and B. Allain.** 1992. Analytical study of avian reticuloendotheliosis virus dimeric RNA generated in vivo and in vitro. J. Virol. **66:**7245–7252.
11. **Darlix, J. L., C. Gabus, M. T. Nugeyre, F. Clavel, and F. Barre-Sinoussi.** 1990. *cis* elements and *trans*-acting factors involved in the RNA dimerization of the human immunodeficiency virus HIV-1. J. Mol. Biol. **216:**689–699.
12. **Götte, M., X. Li, and M. A. Wainberg.** 1999. HIV-1 reverse transcription: a brief overview focused on structure-function relationships among molecules involved in initiation of the reaction. Arch. Biochem. Biophys. **365:**199–210.
13. **Graham, F. L., J. Smiley, W. C. Russell, and R. Nairn.** 1977. Characteristics of a human cell line transformed by DNA from human adenovirus type 5. J. Gen. Virol. **36:**59–74.
14. **Höglund, S., Å. Öhagen, J. Goncalves, A. T. Panganiban, and D. Gabuzda.** 1997. Ultrastructure of HIV-1 genomic RNA. Virology **233:**271–279.
15. **Hu, W. S., and H. M. Temin.** 1990. Retroviral recombination and reverse transcription. Science **250:**1227–1233.
16. **Huthoff, H., and B. Berkhout.** 2001. Mutations in the TAR hairpin affect the equilibrium between alternative conformations of the HIV-1 leader RNA. Nucleic Acids Res. **29:**2594–2600.
17. **Huthoff, H., and B. Berkhout.** 2001. Two alternating structures of the HIV-1 leader RNA. RNA **7:**143–157.
18. **Ikeda, T., H. Nishitsuji, X. Zhou, N. Nara, T. Ohashi, M. Kannagi, and T. Masuda.** 2004. Evaluation of the functional involvement of human immunodeficiency virus type 1 integrase in nuclear import of viral cDNA during acute infection. J. Virol. **78:**11563–11573.
19. **Julias, J. G., A. L. Ferris, P. L. Boyer, and S. H. Hughes.** 2001. Replication of phenotypically mixed human immunodeficiency virus type 1 virions containing catalytically active and catalytically inactive reverse transcriptase. J. Virol. **75:**6537–6546.
20. **Koh, K. B., M. Fujita, and A. Adachi.** 2000. Elimination of HIV-1 plasmid DNA from virus samples obtained from transfection by calcium-phosphate co-precipitation. J. Virol. Methods **90:**99–102.
21. **Marquet, R., F. Baudin, C. Gabus, J. L. Darlix, M. Mougel, C. Ehresmann, and B. Ehresmann.** 1991. Dimerization of human immunodeficiency virus (type 1) RNA: stimulation by cations and possible mechanism. Nucleic Acids Res. **19:**2349–2357.
22. **Marquet, R., J. C. Paillart, E. Skripkin, C. Ehresmann, and B. Ehresmann.** 1994. Dimerization of human immunodeficiency virus type 1 RNA involves sequences located upstream of the splice donor site. Nucleic Acids Res. **22:**145–151.
23. **McBride, M. S., and A. T. Panganiban.** 1996. The human immunodeficiency virus type 1 encapsidation site is a multipartite RNA element composed of functional hairpin structures. J. Virol. **70:**2963–2973.

24. **McBride, M. S., and A. T. Panganiban.** 1997. Position dependence of functional hairpins important for human immunodeficiency virus type 1 RNA encapsidation in vivo. J. Virol. **71:**2050–2058.
25. **McBride, M. S., M. D. Schwartz, and A. T. Panganiban.** 1997. Efficient encapsidation of human immunodeficiency virus type 1 vectors and further characterization of *cis* elements required for encapsidation. J. Virol. **71:** 4544–4554.
26. **Moumen, A., L. Polomack, B. Roques, H. Buc, and M. Negroni.** 2001. The HIV-1 repeated sequence R as a robust hot-spot for copy-choice recombination. Nucleic Acids Res. **29:**3814–3821.
27. **Nagao, T., A. Yoshida, A. Sakurai, A. Piroozmand, A. Jere, M. Fujita, T. Uchiyama, and A. Adachi.** 2004. Determination of HIV-1 infectivity by lymphocytic cell lines with integrated luciferase gene. Int. J. Mol. Med. **14:**1073–1076.
28. **Ohishi, M., T. Shioda, and J. I. Sakuragi.** 2007. Retro-transduction by virus pseudotyped with glycoprotein of vesicular stomatitis virus. Virology **362**: 131–138.
29. **Paillart, J. C., L. Berthoux, M. Ottmann, J. L. Darlix, R. Marquet, B. Ehresmann, and C. Ehresmann.** 1996. A dual role of the putative RNA dimerization initiation site of human immunodeficiency virus type 1 in genomic RNA packaging and proviral DNA synthesis. J. Virol. **70:**8348–8354.
30. **Paillart, J. C., R. Marquet, E. Skripkin, C. Ehresmann, and B. Ehresmann.** 1996. Dimerization of retroviral genomic RNAs: structural and functional implications. Biochimie **78:**639–653.
31. **Paillart, J. C., M. Shehu-Xhilaga, R. Marquet, and J. Mak.** 2004. Dimerization of retroviral RNA genomes: an inseparable pair. Nat. Rev. Microbiol. **2:**461–472.
32. **Paillart, J. C., E. Skripkin, B. Ehresmann, C. Ehresmann, and R. Marquet.** 2002. In vitro evidence for a long range pseudoknot in the 5′-untranslated and matrix coding regions of HIV-1 genomic RNA. J. Biol. Chem. **277:**5995–6004.
33. **Paillart, J. C., E. Skripkin, B. Ehresmann, C. Ehresmann, and R. Marquet.** 1996. A loop-loop "kissing" complex is the essential part of the dimer linkage of genomic HIV-1 RNA. Proc. Natl. Acad. Sci. USA **93:**5572–5577.
34. **Prats, A. C., C. Roy, P. A. Wang, M. Erard, V. Housset, C. Gabus, C. Paoletti, and J. L. Darlix.** 1990. *cis* elements and *trans*-acting factors involved in dimer formation of murine leukemia virus RNA. J. Virol. **64:**774–783.
35. **Rein, A.** 2004. Take two. Nat. Struct. Mol. Biol. **11:**1034–1035.
36. **Roy, C., N. Tounekti, M. Mougel, J. L. Darlix, C. Paoletti, C. Ehresmann, B. Ehresmann, and J. Paoletti.** 1990. An analytical study of the dimerization of in vitro generated RNA of Moloney murine leukemia virus MoMuLV. Nucleic Acids Res. **18:**7287–7292.
37. **Russell, R. S., C. Liang, and M. A. Wainberg.** 2004. Is HIV-1 RNA dimerization a prerequisite for packaging? Yes, no, probably? Retrovirology **1:**23.
38. **Russell, R. S., A. Roldan, M. Detorio, J. Hu, M. A. Wainberg, and C. Liang.** 2003. Effects of a single amino acid substitution within the p2 region of human immunodeficiency virus type 1 on packaging of spliced viral RNA. J. Virol. **77:**12986–12995.
39. **Sakuragi, J., A. Iwamoto, and T. Shioda.** 2002. Dissociation of genome dimerization from packaging functions and virion maturation of human immunodeficiency virus type 1. J. Virol. **76:**959–967.
40. **Sakuragi, J., T. Shioda, and A. T. Panganiban.** 2001. Duplication of the primary encapsidation and dimer linkage region of HIV-1 RNA results in the appearance of monomeric RNA in virions. J. Virol. **75:**2557–2565.
41. **Sakuragi, J., S. Ueda, A. Iwamoto, and T. Shioda.** 2003. Possible role of dimerization in human immunodeficiency virus type 1 genome RNA packaging. J. Virol. **77:**4060–4069.
42. **Sakuragi, J. I., and A. T. Panganiban.** 1997. Human immunodeficiency virus type 1 RNA outside the primary encapsidation and dimer linkage region affects RNA dimer stability in vivo. J. Virol. **71:**3250–3254.
43. **Willey, R. L., D. H. Smith, L. A. Lasky, T. S. Theodore, P. L. Earl, B. Moss, D. J. Capon, and M. A. Martin.** 1988. In vitro mutagenesis identifies a region within the envelope gene of the human immunodeficiency virus that is critical for infectivity. J. Virol. **62:**139–147.
44. **Zuker, M.** 1989. On finding all suboptimal foldings of an RNA molecule. Science **244:**48–52.